NIH Public Access
Author Manuscript
Cancer Res. Author manuscript; available in PMC 2014 December 15.

Published in final edited form as:
Cancer Res. 2013 December 15; 73(24): 7211–7221. doi:10.1158/0008-5472.CAN-13-1314.

TLR9 signaling in the tumor microenvironment initiates cancer recurrence after radiation therapy

Chan Gao[1], **Anna Kozlowska**[1,8], **Sergey Nechaev**[1,7], **Haiqing Li**[2], **Qifang Zhang**[1], **Dewan M. S. Hossain**[1], **Claudia M. Kowolik**[3], **Peiguo Chu**[4], **Piotr Swiderski**[5], **Don J. Diamond**[6], **Sumanta K. Pal**[3], **Andrew Raubitschek**[1], and **Marcin Kortylewski**[1,*]

[1]Department of Cancer Immunotherapeutics & Tumor Immunology, Beckman Research Institute at City of Hope, Duarte, CA 91010, USA [2]Bioinformatics Core Facility, Beckman Research Institute at City of Hope, Duarte, CA 91010, USA [3]Department of Medical Oncology, Beckman Research Institute at City of Hope, Duarte, CA 91010, USA [4]Department of Pathology, Beckman Research Institute at City of Hope, Duarte, CA 91010, USA [5]DNA/RNA Synthesis Core Facility, Beckman Research Institute at City of Hope, Duarte, CA 91010, USA [6]Division of Translational Vaccine Research, Beckman Research Institute at City of Hope, Duarte, CA 91010, USA [7]Irell & Manella Graduate School of Biological Sciences, Beckman Research Institute at City of Hope, Duarte, CA 91010, USA [8]Medical Biotechnology, University of Medical Sciences, Poznan, Poland

Abstract

Cancer radiotherapy may be immunogenic, but it is unclear why its immunogenic effects are rarely sufficient to prevent tumor recurrence. Here we report a novel Toll receptor-9 (TLR9)-dependent mechanism that initiates tumor regrowth after local radiotherapy. Systemic inhibition of TLR9, but not TLR4, delayed tumor recurrence in mouse models of B16 melanoma, MB49 bladder cancer and CT26 colon cancer after localized high-dose tumor irradiation. Soluble factors in the microenvironment of regressing tumors triggered TLR9 signaling in freshly recruited myeloid cells appearing within four days of radiotherapy. The tumorigenic effects of TLR9 depended on MyD88/NF-κB-mediated upregulation of IL-6 expression, which in turn resulted in downstream activation of Jak/STAT3 signaling in myeloid cells. By comparing global gene expression in wild-type, TLR9- or STAT3-deficient myeloid cells derived from irradiated tumors, we identified a unique set of TLR9/STAT3-regulated genes involved in tumor-promoting inflammation and re-vascularization. Blocking STAT3 function by two myeloid-specific genetic strategies corrected TLR9-mediated cancer recurrence after radiation therapy. Our results suggest that combining localized tumor irradiation with myeloid cell-specific inhibition of TLR9/STAT3 signaling may help eliminate radiation-resistant cancers.

[*]Corresponding Author : Marcin Kortylewski, Ph. D., Beckman Research Institute at City of Hope, Duarte, CA 91010, USA, mkortylewski@coh.org; phone: (626) 256-4673, ext.64120; fax: (626) 471-3602.

No potential conflicts of interest were disclosed.

AUTHORS' CONTRIBUTIONS

Conception and design: C.Gao, M.Kortylewski
Acquisition of data: C.Gao, A.Kozlowska, S.Nechaev, M.Kortylewski
Analysis and interpretation of data: C.Gao, A.Kozlowska, H Li, P.Chu, A.Raubitschek, M.Kortylewski
Writing and/or review of the manuscript: C.Gao, S.Nechaev, C.M.Kowolik, S.K.Pal, A.Raubitschek, D.J.Diamond, M.Kortylewski
Technical and/or material support: Q.Zhang, D.M.S.Hossain, C.M.Kowolik, P.Swiderski
Study supervision: M.Kortylewski

NIH-PA Author Manuscript
NIH-PA Author Manuscript
NIH-PA Author Manuscript

NIH-PA Author Manuscript

NIH-PA Author Manuscript

NIH-PA Author Manuscript

Keywords

TLR9; IL-6; STAT3; tumor; radiotherapy

INTRODUCTION

Radiation therapy (RT) relies on the increased radiation sensitivity of proliferating cells in comparison to surrounding patient tissues. As a non-invasive strategy, RT became one of the primary treatment modalities for about half of all cancer patients (1, 2). However, many cancer types, such as melanoma, renal carcinoma or advanced prostate cancers, are considered either completely or partly radioresistant (1, 2). More recently, emerging data has shown that long-term effects of RT are limited by intrinsic radioresistance of cancer cells and by extrinsic influence of the tumor stroma (3–5). Several tumor-associated but non-malignant cell populations, including endothelial cells (6) and myeloid immune cells (7, 8), were implicated in promoting tumor recurrence after RT. Recent studies demonstrated that, within a few days after irradiation, regressing tumors recruit inflammatory monocytes/macrophages from the bone-marrow (7–10). Tumor-associated macrophages (TAMs) and other $CD11b^+$ myeloid cell populations are known for supporting tumor growth, invasion, metastasis and immune evasion (11–14). The $CD11b^+$ monocytes recruited into the injured tissue can also recognize components of dying cells, which include TLR agonists (11, 15, 16). However, despite the abundance of immunostimulatory molecules, tumors frequently reoccur even after high dose irradiation (17). Recent studies suggested that these undesirable effects may depend on myeloid cells, which stimulate restoration of tumor blood vessel after radiation-induced damage (9). However, the molecular mechanism(s) underlying tumor recurrence after radiotherapy were not defined.

Toll-like receptors (TLRs) play crucial roles in driving inflammatory responses of myeloid cells in reaction to tissue stress and injury (11, 18, 19). TLR signaling is tightly controlled by multiple and interconnected layers of negative regulatory pathways (20). Signal transducer and activator of transcription 3 (STAT3) seems to play a central role in the regulation of TLR-induced inflammatory processes in normal wound healing and in tumorigenesis (20, 21). Previous studies revealed that STAT3 is a negative feedback inhibitor for proinflammatory signaling by TLR4 and TLR9 in myeloid cells (22, 23). In addition, STAT3 activation was shown to enhance angiogenic activity of myeloid cells, while limiting antigen presentation (24, 25). Persistent STAT3 activity within the tumor microenvironment results from stimulation by cytokines, growth factors and sphingolipids secreted by cancer and tumor stroma cells (20, 21). High-dose tumor RT eliminates the majority of cancer cells and tumor-associated stroma, disrupting the immunosuppressive signaling network and generating potentially immunogenic signals. However, it ultimately fails to prevent tumor regrowth. In the current study, we investigated whether local triggering of innate immunity receptors, such as TLR9, can provide an emergency tumorigenic signal to jump-start tumor regrowth after RT.

MATERIALS AND METHODS

In vivo experiments

Mouse B16 and CT26 cells were from American Type Culture Collection; MB49 cells were generous gift from T. Ratliff (University of Iowa) and were kept in culture for less than 6 months. Cells were not further authenticated. *Tlr4*$^{-/-}$ mice were obtained from the Jackson Laboratory, while *Tlr9*$^{-/-}$ mice were originally from S. Akira (Osaka University). Generation of mice with *Stat3*$^{-/-}$ hematopoietic cells using inducible *Mx1-Cre* system was reported previously (33). Mice were backcrossed for 7–10 generations to make them

NIH-PA Author Manuscript

NIH-PA Author Manuscript

NIH-PA Author Manuscript

C57BL/6 congenic. To generate poly(I:C)-inducible *MyD88*$^{-/-}$ mouse model, C57BL/6 *MyD88*$^{loxP/loxP}$ and *Mx1-Cre* mice (JacksonLabs) were crossed to generate *Mx1-Cre/MyD88*$^{loxP/loxP}$ mice. Animal care was performed under pathogen-free conditions following approved protocols from Institutional Animal Care and Use Committees (COH). Established *s.c.* tumors were irradiated using single collimated dose of radiation from Cs-137 source using MARK-I irradiator (J.L.Shepherd). The radiation was 13.3Gy (±0.5 Gy) at the tumor site and negligible (0.01–0.16 Gy) in the 1 cm distance as measured using dosimeters (n = 4). Mice were injected peritumorally with CpG-siRNA (1mg/kg) or retroorbitally with TTAGGG ODN (5mg/kg) every other day. Oligonucleotides were synthesized in the DNA/RNA Synthesis Core at COH; the design of CpG-siRNA was described (35, 50). Spleen or tumor tissues were dissociated to single cell suspensions as reported before (33). For Matrigel experiments, CD11b^{+}CD11c^{-} cells were enriched from spleens of WT or *Tlr9*$^{-/-}$ tumor-bearing mice with over 90% purity using magnetic separation (Stem Cell Technologies). 1×10^{6} WT or *Tlr9*$^{-/-}$ myeloid cells were admixed with 1×10^{5} B16 cells in growth factor–reduced Matrigel (BD Biosciences) and injected into WT mice. After 6d, Matrigel plugs were removed for hemoglobin analysis using Drabkin's reagent (Sigma-Aldrich).

Immunofluorescent staining

Flash-frozen tumor specimens were fixed and stained with antibodies specific to myeloid (CD11b), endothelial (MECA32) and endothelial progenitor cells (VEGFR2) (BD), then detected with fluorochrome-coupled secondary antibodies (Invitrogen) as described (33).

Western blotting

Cells were treated with supernatants from *in vivo* irradiated tumors following the pre-treatment with 10 nM NF-κB inhibitor (EMD481407; Millipore) or with neutralizing antibodies to IL-6 (10 μg/ml; BD). Total cellular lysates were prepared as previously reported (33) and analyzed using antibodies specific to tyrosine phosphorylated STAT3 (Cell Signaling), total STAT3 (Santa Cruz) and β-actin (Sigma-Aldrich).

Quantitative real-time PCR

Total RNA was extracted from primary cells using mirVana™ miRNA Isolation Kit (Ambion) and then transcribed them into cDNAs with RT^{2} First Strand Kit (Qiagen). The qPCR was carried out using primers for *Il6* (Qiagen) using CFX96 Real-Time PCR Detection System (Bio-Rad).

Global gene expression analysis

Total RNA samples extracted from magnetically-enriched tumor-infiltrating CD11b^{+} cells using mirVana™ Isolation Kit (Ambion) were sequenced on Illumina HiSeq2000. Sequences that passed the default chastity filter were aligned with the mouse reference genome (Genome Browser, UCSC, CA) using the TopHat software v.1.3.1 to identify differential gene expression. The results were converted to reads/kilo base of total exon length/million mapped (RPKM) reads using GenomicsSuite v.6.12.0713 (Partek) and normalized to gene models in the NCBI RefSeq database with a stringent cutoff of 0.1 RPKM and the false discovery rate (FDR) < 0.05. Differentially expressed mRNA had fold change cutoff of 1.5 and *P*-value with FDR cutoff of 0.05. The expression profiling data were submitted to the Gene Expression Omnibus (GSE45180).

Flow cytometry

For extracellular immunostaining, single cell suspensions were incubated with fluorochrome-coupled antibodies to CD11b and Gr1 (BD). Prior to intracellular staining for

NIH-PA Author Manuscript

NIH-PA Author Manuscript

NIH-PA Author Manuscript

tyrosine-phosphorylated STAT3 (BD), cells were fixed and permeated as described (33). Fluorescence data were analyzed using Accuri C6 cytometer (BD) and FlowJo software v. 7.6.5 (Tree Star).

Statistics

Unpaired t test was used to calculate two-tailed *P* value to estimate statistical significance of differences between two treatment groups. One- or two-way ANOVA plus Bonfeerroni post-test were applied to assess differences between multiple groups or in tumor growth kinetics experiments, respectively. Statistically significant *P* values were indicated in figures as follows: **, $P < 0.01$ and *, $P < 0.05$. Data were analyzed using Prism software v. 4.0 (GraphPad).

RESULTS

TLR9 triggering initiates tumor regrowth after local radiation therapy

TLR4 and TLR9 are reportedly involved in responses to tissue injury (11, 15), therefore we assessed whether genetic ablation of either one of these receptors will influence the effect of local RT. Wild-type (WT), *Tlr4*$^{-/-}$ or *Tlr9*$^{-/-}$ mice were injected *s.c.* with B16 melanoma cells which are highly radioresistant tumors (26). After tumors were established (average diameter 8–10mm), mice were treated with a single 13Gy dose of radiation focally directed to the tumor site. Unexpectedly, *Tlr9* deletion did not accelerate but instead significantly delayed the regrowth of B16 tumors post-RT compared to WT mice. In contrast, B16 tumors in *Tlr4*$^{-/-}$ mice grew with similar kinetics as in controls (Figure 1A). We found an even more pronounced effect of *Tlr9* gene deletion on the recurrence of irradiated MB49 bladder carcinomas. The single dose of irradiation induced complete regression of MB49 tumors in the majority of *Tlr9*-deficient mice, while only transiently inhibiting MB49 growth in WT mice (Figure 1B). The *Tlr*-deficient and control wild-type C57BL/6 mice were congenic to limit the influence of genetic differences. We also verified these results in wild-type C57BL/6 and Balb/C mice using the TLR9 receptor antagonist, TTAGGG oligodeoxynucleotide (ODN) (27). Repeated intravenous injections of TLR9 antagonist significantly delayed recurrence of B16 (Figure 1C), MB49 (Figure 1D) or CT26 colorectal carcinoma (Figure 1E) tumors in C57BL/6 or Balb/C mice, respectively. These results suggest that independently from the mouse genetic background, TLR9 triggering in the tumor microenvironment provides a common mechanism promoting tumor recurrence after RT.

TLR9 supports reconstruction of tumor blood vessels after radiation therapy

To understand the role of TLR9 in promoting tumor growth after RT, we first evaluated the rate of B16 tumor re-vascularization in WT and *Tlr9*$^{-/-}$ mice. We compared the average size of blood vessels formed in WT and *Tlr9*$^{-/-}$ mice within 10d after tumor irradiation. At this time the average tumor volumes in both experimental groups were comparable, which allowed for the analysis of blood vessels before tumor regrowth usually occuring in the WT group by 12d post-RT. For unbiased assessment, we quantified fluorescently stained MECA32^{+} endothelial cells on whole tumor cross sections using automated slide scanning (Figure 2A and Supplementary Figure 1). The analysis of WT and *Tlr9*$^{-/-}$ B16 tumor cross-sections revealed that tumor blood vessels in *Tlr9*$^{-/-}$ mice were small and mostly immature, in contrast to well-developed tumor vasculature in WT mice (Figure 2A). The average blood vessel size in *Tlr9*$^{-/-}$ mice compared to WT controls was reduced 3-fold (Figure 2B). Recent studies linked formation of tumor vasculature to the recruitment of endothelial progenitor cells (EPCs) from the bone marrow which usually occurs 4d after tumor irradiation (9). To verify whether EPCs can contribute to poor tumor revascularization in *Tlr9*-ablated mice, we assessed VEGFR2^{+} EPCs in tumors early (day 4) and late (day 10) after RT. The immunofluorescent microscopy revealed that transient tumor infiltration by

NIH-PA Author Manuscript

NIH-PA Author Manuscript

NIH-PA Author Manuscript

EPCs occurs at 4d after irradiation only in WT but not in *Tlr9*$^{-/-}$mice (Figures 2C and 2D). At 10d post-RT, EPCs were rare in tumors from both groups. Our results suggest that transient EPC mobilization preceded restoration of tumor vasculature after radiation-induced tumor cell death.

TLR9 signaling in myeloid cells promotes revascularization of irradiated tumors

Bone marrow-derived myeloid cells support early stages of tumor growth (11, 28) and ionizing radiation is known to intensify the process of their recruitment (9). The microscopic examination of immunofluorescently stained B16 tumor sections showed increased numbers of CD11b^{+} myeloid cells in tumors at day 4 after irradiation compared to non-irradiated controls in both WT and *Tlr9*$^{-/-}$ mice (Supplementary Figure 2A). To assess percentages of tumor-infiltrating myeloid cells, we analyzed single cell suspensions from whole tumors with or without prior irradiation using flow cytometry. As expected, numbers of tumor-infiltrating CD11b^{+} cells were significantly increased 4d after irradiation (Figure 3A). Most of the freshly recruited cells were CD11b^{+}Gr1^{-} macrophages with smaller percentages of CD11b^{+}Gr1^{+} immature myeloid cells.

Previous studies demonstrated that pro-angiogenic activity of TAMs and other myeloid cells largely depends on signaling by STAT3 (11, 24, 25). We therefore assessed whether *in vivo* TLR9 signaling can activate STAT3 in myeloid cells mobilized into irradiated B16 tumors. FACS analysis of activated, tyrosine-phosphorylated STAT3 (pSTAT3), showed elevated levels of pSTAT3 in TAMs from WT but not from *Tlr9*$^{-/-}$ mice at day 4 post-RT (Figure 3B). Similar effects were observed also in immature myeloid cells (CD11b^{+}Gr1^{+}), although the overall levels of STAT3 phosphorylation were lower than in macrophages (Supplementary Figure 2B). We further verified these data using sorted immune cell populations from *in vivo* irradiated tumors as well as on *in vitro*-treated splenocytes (Supplementary Fig. 3C–E). Altogether, our results indicate that in the microenvironment of irradiated tumor, TLR9 activates STAT3 signaling specifically in CD11b^{+}F4/80^{+} TAMs. To verify whether TLR9^{+}/pSTAT3^{+} tumor-associated myeloid cells play pro-vasculogenic/angiogenic role in the irradiated tumor microenvironment, we performed *in vivo* Matrigel plug assays. Splenic CD11b^{+} cells isolated from B16 tumor-bearing WT or *Tlr9*$^{-/-}$ mice were suspended in supernatant derived from *in vivo* irradiated tumors, admixed with B16 cells in Matrigel and injected *s.c.* into mice. Six days later, Matrigel plugs were harvested to assess formation of early blood vessels and measure the hemoglobin content which corresponds with the extent of neovascularization. Matrigel plugs containing WT myeloid cells showed significantly increased hemoglobin levels compared to Matrigel plugs with *Tlr9*$^{-/-}$ myeloid cells (Figure 3C). Our control experiments confirmed that under the same experimental conditions vascularization of Matrigel plugs with B16 tumors is increased nearly twice by WT myeloid cells (Supplementary Figure 2C). These results indicate that TLR9 expression is required for myeloid cell-specific STAT3 activation as well as for the tumor revascularization after RT.

IL-6 couples TLR9 to STAT3 signaling in myeloid cells accumulated in irradiated tumors

Next, we assessed whether soluble factors released from *in vivo* irradiated tumors can stimulate TLR9-mediated STAT3 activity in normal myeloid cells. The B16 tumors established in C57BL/6 mice were locally irradiated as described in Figure 1. After 4d tumors were harvested and gently dispersed into single cell suspensions. The soluble fractions collected from irradiated or non-irradiated B16 tumor suspensions were then used to treat freshly isolated WT or *Tlr9*$^{-/-}$ splenocytes. As shown in Figure 4A, supernatants from *in vivo* irradiated B16 tumors were more potent in inducing STAT3 phosphorylation in WT splenocytes than supernatants from non-irradiated tumors. In contrast, *Tlr9* gene deletion abrogated STAT3 activation (Figure 4A). Similar effect was observed using

NIH-PA Author Manuscript

NIH-PA Author Manuscript

NIH-PA Author Manuscript

supernatants derived from a different tumor model, CT26 colon carcinoma, in both *Tlr9*$^{-/-}$ but not WT or *Tlr4*$^{-/-}$ splenocytes (Supplementary Figure 3A). To verify whether STAT3 activation is induced by soluble TLR9 ligands present in tumor supernatants, we used a competitive TLR9 inhibitor (TTAGGG) as in Figure 1. The specific TLR9 blocking prevented upregulation of pSTAT3 in splenocytes treated using irradiated B16 tumor supernatant (Figure 4B and Supplementary Figure 3B). In contrast, the TLR9 inhibitor did not affect STAT3 activation induced by supernatant derived from non-irradiated B16 tumors. This is consistent with the well known role of multiple cytokines and growth factors in stimulating STAT3 activity in the intact tumor microenvironment (29).

To understand the molecular mechanism(s) leading to STAT3 activation in the irradiated tumor microenvironment, we first assessed whether these effects depend on MyD88, a critical adaptor molecule downstream from TLR9 (30). We have generated mice with inducible deletion of MyD88 in all hematopoietic cells, including myeloid CD11b^{+} cells (*Mx1-Cre/MyD88*$^{loxP/loxP}$). As shown in Fig. 4C, STAT3 activation by supernatants derived from irradiated tumors was reduced in splenic CD11b^{+} cells from MyD88-deficient compared to WT mice. We further verified that STAT3 induction through TLR9/MyD88 signaling involves NF-κB. In fact, small molecule NF-κB inhibitor abrogated STAT3 activation by the irradiated tumor supernatant in primary myeloid cells (Fig. 4D). Our initial studies indicated that TLR9 stimulation leads to release of soluble factor(s) that activates STAT3 in target cells (Supplementary Figure 4A). TLR9/MyD88/NF-κB signaling is known to induce expression of numerous soluble proinflammatory mediators, which are expressed rapidly after stimulation and can activate STAT3 (31, 32). In addition, our *in vitro* experiments on splenocytes indicated that STAT3 activation is sensitive to broad specificity Janus kinases (Jak) inhibitors (Supplementary Figure 4B). Further gene expression analysis using qPCR identified that TLR9/NF-κB signaling in immune cells upregulates IL-6 expression, which is as a potent activator of STAT3 signaling (Figure 4E and Supplementary Figure 4C) (32). We confirmed these results using tumor supernatants from both irradiated and non-irradiated tumors. As shown in Figure 4F, the antibody-mediated neutralization of IL-6 in irradiated tumor supernatants reduced STAT3 activation in splenocytes. In contrast, blocking IL-6 had lesser effect on STAT3 activation by non-irradiated supernatants. The neutralization of type I IFNs, which are also upregulated by TLR9 signaling, did not prevent STAT3 activation (Supplementary Figure 4D) (30). These results suggest that IL-6 bridges signaling from TLR9 to Jak/STAT3 in myeloid cells accumulated in tumors after RT.

TLR9/STAT3 signaling orchestrates tumorigenesis-promoting gene expression in myeloid cells

Our results uncovered a potential molecular mechanism jump-starting tumor recurrence after RT. To assess whether STAT3 plays a role in these TLR9-induced effects, we compared global gene expression in CD11b^{+} myeloid cells isolated from tumors irradiated in genetically matched WT, *Tlr9*- and *Stat3*-deficient C57BL/6 mice (33). The expression levels of over 22,000 transcripts were analyzed in RNA samples from 3–4 individual mice sequenced on Illumina HiSeq2000. Genes that were differentially expressed in comparison to WT with a stringency cutoff of *FDR* < 0.05 were identified as regulated either by TLR9 or STAT3. The hierarchical clustering of differentially expressed genes in individual mice revealed molecular signatures for WT, *Tlr9*$^{-/-}$ and *Stat3*$^{-/-}$ groups of mice (Figure 5A), while confirming the specificity of TLR9 and STAT3 gene ablation (Supplementary Figure 5A and data not shown). Differentially regulated (> 1.5 fold) transcripts found in *Stat3*$^{-/-}$ myeloid cells (2145 up- and 786 down-regulated) were twice the number of transcripts identified in *Tlr9*$^{-/-}$ cells (1165 up- and 343 down-regulated), thus underscoring the role of *Stat3* as a point of convergence for tumorigenic signaling networks in immune cells (Figure

NIH-PA Author Manuscript

NIH-PA Author Manuscript

NIH-PA Author Manuscript

5B) (20, 29). Importantly, in comparison to WT controls, 993 transcripts were commonly regulated in *Tlr9*$^{-/-}$ and *Stat3*$^{-/-}$ myeloid cells (796 up- and 197 down-regulated) (Figure 5B). These results suggest that STAT3 is directly or indirectly involved in the transcription of 68% (796/1165) of all negatively, or 57% (197/343) of all positively TLR9-regulated genes during tumor regrowth post-RT.

Top functional gene categories common for *Tlr9*$^{-/-}$ and *Stat3*$^{-/-}$ tumor-associated myeloid cells are likely related to cellular growth, survival, angiogenesis and inflammatory immune responses as suggested by the Ingenuity Pathway Analysis software (IPA) (Figure 5C). Among the transcripts downregulated in *Tlr9*$^{-/-}$ and *Stat3*$^{-/-}$myeloid cells compared to WT cells, were many genes known for promoting tumorigenic inflammation and angiogenesis, including *Il6, Il6st, Il23, Lif, Hbegf, Ccl1* and its receptor (*Ccr8*), *Hdc*, *S1pr3*, *Plaur*, *Trem1* and *Tgfb1* (Figure 5D). Several of these genes encoded soluble ligands or receptors, which are known as activators of STAT3 signaling (IL-6/IL-6R, IL-23, LIF, S1PR3, HBEGF) (21). In contrast, the expression of several mediators of innate and adaptive antitumor immunity such as *Ifnb*, *Il15* and *Il18* was elevated in *Tlr9*$^{-/-}$ and *Stat3*$^{-/-}$myeloid cells compared to WT cells (Figure 5E).

The other prominent functional gene category targeted by TLR9/STAT3 signaling comprised several transcription factor genes critical for monocyte/macrophage differentiation. Tumorigenic genes which are activated in macrophages under hypoxia, such as *Ets2* oncogene, as well as *Egr1, Egr3* (34), were reduced in *Tlr9*- and *Stat3*-deficient myeloid cells compared to WT controls. In contrast, several genes promoting terminal differentiation and growth arrest (*Gadd45a, Gadd45b, Gadd45g, Rock1*) or apoptosis (*Bclaf1, Pdcd5, Tmf1*) were elevated in *Tlr9*- and *Stat3*-deficient macrophages. Several genes selected based on RNA sequencing data were validated using qPCR (Supplementary Figure 5B). These results suggest that STAT3 signaling downstream from TLR9 allows for concerted regulation of myeloid cell differentiation, survival and proangiogenic activity in tumors recurring after RT.

Targeting STAT3 in TLR9^{+} myeloid cells augments the efficacy of local tumor irradiation

We next assessed whether blocking STAT3 in the myeloid compartment would compromise tumor regrowth following local RT. B16 cells were injected into littermate mice with or without deletion of *Stat3* in myeloid cells. At 8d, tumors established in both *Stat3*$^{+/+}$ and *Stat3*$^{-/-}$ mice (average volume of 34 mm^3) were treated locally irradiated or left untreated. As shown in Figure 6A, the combination of *Stat3* ablation in myeloid cells with RT effectively prevented tumor regrowth. *Stat3* deletion alone and tumor irradiation alone delayed, though did not abrogate B16 tumor growth. Mice with prolonged (>4 weeks) *Stat3* ablation in hematopoietic cells develop autoinflammatory disorders which limit experimental timeframe (33). Thus, we decided to use CpG-*Stat3* siRNA as an alternative strategy to target STAT3 specifically in TAMs. We previously demonstrated that siRNA conjugated to CpG ODNs are actively internalized by TLR9-positive cells and induce gene silencing in both mouse and human systems (35). Mice with established B16 tumors (average volume of 198 mm^3) were injected peritumorally using CpG-*Stat3* siRNA or control non-targeting CpG-*Luc* siRNA every other day. To reduce STAT3 protein, treatments were started 2d before RT. We did not observe tumor growth inhibition after RT alone or after control CpG-*Luc* siRNA treatment (Figure 6B). This was likely a result of increased radioresistance of large tumors (2). However, CpG-*Stat3* siRNA treatment combined with RT resulted in tumor growth arrest in the majority of mice (Figure 6B).

NIH-PA Author Manuscript

NIH-PA Author Manuscript

NIH-PA Author Manuscript

DISCUSSION

Recent clinical reports indicated that radiotherapy has the potential to generate abscopal effects and systemic antitumor immunity (36). Paradoxically, tumor irradiation was also shown to enhance cancer cell repopulation and recurrence (8, 10, 37). Our study reconciles these observations identifying a novel molecular mechanism which controls the outcome of RT. We demonstrate that TLR9, the innate immune receptor, triggers MyD88/NF-κB-mediated expression of IL-6, which in turn induces tumorigenic signaling in myeloid cells freshly recruited in response to tumor irradiation (Figure 7). We show that tumorigenic activity of $TLR9^+$ myeloid cells depends on the IL-6-induced activation of STAT3, a master regulator of tumor angiogenesis and immune evasion (21). We demonstrate for the first time that the TLR9/IL-6/STAT3 signaling axis promotes expression of a unique set of genes in myeloid cells that contribute to neovascularization of irradiated tumors.

Our studies provide evidence that TLR9 activation in myeloid cells depends on soluble factors released into the tumor microenvironment after irradiation. Blocking TLR9 stimulation with an antagonistic oligonucleotide mimicked the effect of *Tlr9* ablation both *in vitro* and *in vivo*. These results agree with recent studies demonstrating that sterile tissue injury can cause TLR9-mediated inflammatory responses *in vivo* (38, 39). *TLR9* gene expression is also the most sensitive to cellular stress caused by DNA damage through ionizing radiation or chemotherapy of all *TLR* gene family members (40). Although *TLR9* expression in humans is more restricted than in mice, recent studies reported TLR9 expression in activated immune cells, such as monocyte-derived DCs, macrophages or neutrophils (31, 41). In agreement with this study, we also observed upregulation of TLR9 levels in lymph node macrophages from cancer patients that underwent radiotherapy compared to tumor-free individuals (Supplementary Figure 6). Whether there is a causal relationship between TLR9 expression and STAT3 activation in human system remains to be established in more extensive studies.

Recent reports suggested that the endogenous trigger for TLR9 signaling might be mitochondrial DNA released from dying cells during injury (38, 39). Whether mitochondrial DNA acts in the naked form or complexed with DNA-binding molecules, such as HMGB1, is still unclear (42, 43). Other nucleic acid receptors, such as RNA-sensing TLR7/8 but not TLR3, could also contribute to the tumorigenic effect of RT through STAT3 activation (Gao/Kortylewski, unpublished data). We found TLR9 ligands in the tumor microenvironment post-RT but not before irradiation. Tumor damage after RT can disintegrates the cytokine/growth factor network which sustains STAT3 activity in growing and established tumors (20, 21). TLR9 triggering is likely to jump-start tumorigenic signaling in newly recruited myeloid cells. Our antibody-mediated neutralization experiments suggest that IL-6 is a critical STAT3 activator present in the irradiated tumor microenvironment. IL-6 is known for inducing rapid STAT3 phosphorylation through the IL-6R-associated Janus family kinases, primarily Jak1 rather than Jak2 or Tyk2 (32). Correspondingly, our *in vitro* experiments using various kinase inhibitors indicated that STAT3 activity was sensitive to broadly specific Jak inhibitors, but it was unaffected by targeting Jak2 only, EGFR, PI3K/Akt or MEK/MAPK. The crucial role of IL-6 in the inflammation-driven carcinogenesis is well established (44). Secretion of IL-6 by monocytes/macrophages translates initial inflammatory responses into tumorigenic STAT3 signaling in both malignant and immune cells. Previous studies performed in tumor-free mice indicated the dominant role of IFNγ- and TNFα-dependent gene expression downstream of TLR9 (45). Our results demonstrate that in TAMs TLR9 signaling is skewed towards IL-6 and STAT3-dependent gene regulation. In addition to IL-6, we uncovered multiple potential STAT3 activators, such as *Lif*, *Il23*, *Hbgef* or *S1pr3*. It is likely that IL-6 initiates a feed-forward mechanism that restores and maintains STAT3 activity by

NIH-PA Author Manuscript

NIH-PA Author Manuscript

NIH-PA Author Manuscript

multidirectional stimulation (21). Furthermore, TLR9/STAT3 signaling coordinates expression of genes supporting angiogenesis, such as *Ets2* (46), and repression of genes involved in macrophage differentiation and apoptosis (47). TLR9/STAT3 signaling was critical for tumor-promoting functions of $CD11b^+$ cells, potentially through the recruitment of $VEGFR2^+$ EPCs. Previous reports demonstrated the role of EPCs in tumor vasculogenesis after irradiation or under normal conditions (8, 28, 48). Nevertheless, we cannot rule out that residual endothelial cells also contribute to the reconstruction of tumor vasculature as suggested by others (9).

The proof-of-principle experiments in mice using both genetic *Stat3* deletion and CpG-*Stat3* siRNA approach confirmed the negative role of TLR9/STAT3 signaling in determining the outcome of RT. Targeting STAT3 in myeloid cells augmented the proinflammatory effect of TLR9 triggering after RT, thereby preventing tumor recurrence. Recent phase I/II study in B cell lymphoma demonstrated that intratumoral injections of CpG ODN can synergize with the effect of radiotherapy emphasizing the need for combination strategies (2, 49). Collectively, these findings imply that myeloid cell-specific inhibition of TLR9/IL-6/Jak/STAT3 signaling can generate novel, safer and more effective strategies to support cancer radiotherapy.

Supplementary Material

Refer to Web version on PubMed Central for supplementary material.

Acknowledgments

We thank Drs. Hua Yu, Behnam Badie, Kim Blenman (COH) for advice and stimulating discussions and to Robbin Newlin (Sanford-Burnham Institute) for assistance with whole slide scanning. We would like to acknowledge the dedication of staff members at the Light Microscopy, Analytical Cytometry Cores and Animal Resource Center (COH).

GRANT SUPPORT

This work was supported by Margaret E.Early Medical Trust Research Grant, STOP CANCER Allison Tovo-Dwyer Memorial Career Development Award (to M.K.) and by the National Cancer Institute of the National Institutes of Health under grants numbers R01CA155367 (to M.K.) and P30CA033572 (to COH). The content is solely the responsibility of the authors and does not necessarily represent the official views of the NIH.

References

1. Bernier J, Hall EJ, Giaccia A. Radiation oncology: a century of achievements. Nat Rev Cancer. 2004; 4:737–47. [PubMed: 15343280]
2. Begg AC, Stewart FA, Vens C. Strategies to improve radiotherapy with targeted drugs. Nat Rev Cancer. 2011; 11:239–53. [PubMed: 21430696]
3. Zhang B, Bowerman NA, Salama JK, Schmidt H, Spiotto MT, Schietinger A, et al. Induced sensitization of tumor stroma leads to eradication of established cancer by T cells. J Exp Med. 2007; 204:49–55. [PubMed: 17210731]
4. Formenti SC, Demaria S. Systemic effects of local radiotherapy. The lancet oncology. 2009; 10:718–26. [PubMed: 19573801]
5. Karar J, Maity A. Modulating the tumor microenvironment to increase radiation responsiveness. Cancer biology & therapy. 2009; 8:1994–2001. [PubMed: 19823031]
6. Garcia-Barros M, Paris F, Cordon-Cardo C, Lyden D, Rafii S, Haimovitz-Friedman A, et al. Tumor response to radiotherapy regulated by endothelial cell apoptosis. Science. 2003; 300:1155–9. [PubMed: 12750523]
7. Ahn GO, Tseng D, Liao CH, Dorie MJ, Czechowicz A, Brown JM. Inhibition of Mac-1 (CD11b/CD18) enhances tumor response to radiation by reducing myeloid cell recruitment. Proc Natl Acad Sci U S A. 2010; 107:8363–8. [PubMed: 20404138]

NIH-PA Author Manuscript

NIH-PA Author Manuscript

NIH-PA Author Manuscript

8. Kioi M, Vogel H, Schultz G, Hoffman RM, Harsh GR, Brown JM. Inhibition of vasculogenesis, but not angiogenesis, prevents the recurrence of glioblastoma after irradiation in mice. J Clin Invest. 2010; 120:694–705. [PubMed: 20179352]
9. Kozin SV, Duda DG, Munn LL, Jain RK. Neovascularization after irradiation: what is the source of newly formed vessels in recurring tumors? J Natl Cancer Inst. 2012; 104:899–905. [PubMed: 22572994]
10. Kozin SV, Kamoun WS, Huang Y, Dawson MR, Jain RK, Duda DG. Recruitment of myeloid but not endothelial precursor cells facilitates tumor regrowth after local irradiation. Cancer Res. 2010; 70:5679–85. [PubMed: 20631066]
11. Murray PJ, Wynn TA. Protective and pathogenic functions of macrophage subsets. Nat Rev Immunol. 2011; 11:723–37. [PubMed: 21997792]
12. Sansone P, Bromberg J. Environment, inflammation, and cancer. Current opinion in genetics & development. 2011; 21:80–5. [PubMed: 21144738]
13. Kuraishy A, Karin M, Grivennikov SI. Tumor promotion via injury- and death-induced inflammation. Immunity. 2011; 35:467–77. [PubMed: 22035839]
14. Goldszmid RS, Trinchieri G. The price of immunity. Nat Immunol. 2012; 13(10):932–8. [PubMed: 22990891]
15. Kono H, Rock KL. How dying cells alert the immune system to danger. Nat Rev Immunol. 2008; 8:279–89. [PubMed: 18340345]
16. Krysko DV, Garg AD, Kaczmarek A, Krysko O, Agostinis P, Vandenabeele P. Immunogenic cell death and DAMPs in cancer therapy. Nat Rev Cancer. 2012; 12:860–75. [PubMed: 23151605]
17. Roses RE, Xu M, Koski GK, Czerniecki BJ. Radiation therapy and Toll-like receptor signaling: implications for the treatment of cancer. Oncogene. 2008; 27:200–7. [PubMed: 18176601]
18. Trinchieri G, Sher A. Cooperation of Toll-like receptor signals in innate immune defence. Nat Rev Immunol. 2007; 7:179–90. [PubMed: 17318230]
19. Murray PJ. NOD proteins: an intracellular pathogen-recognition system or signal transduction modifiers? Curr Opin Immunol. 2005; 17:352–8. [PubMed: 15950446]
20. Murray PJ, Smale ST. Restraint of inflammatory signaling by interdependent strata of negative regulatory pathways. Nat Immunol. 2012; 13:916–24. [PubMed: 22990889]
21. Yu H, Pardoll D, Jove R. STATs in cancer inflammation and immunity: a leading role for STAT3. Nat Rev Cancer. 2009; 9:798–809. [PubMed: 19851315]
22. Vicari AP, Chiodoni C, Vaure C, Ait-Yahia S, Dercamp C, Matsos F, et al. Reversal of tumor-induced dendritic cell paralysis by CpG immunostimulatory oligonucleotide and anti-interleukin 10 receptor antibody. J Exp Med. 2002; 196:541–9. [PubMed: 12186845]
23. Kortylewski M, Kujawski M, Herrmann A, Yang C, Wang L, Liu Y, et al. Toll-like receptor 9 activation of signal transducer and activator of transcription 3 constrains its agonist-based immunotherapy. Cancer Res. 2009; 69:2497–505. [PubMed: 19258507]
24. Kujawski M, Kortylewski M, Lee H, Herrmann A, Kay H, Yu H. Stat3 mediates myeloid cell-dependent tumor angiogenesis in mice. J Clin Invest. 2008; 118:3367–77. [PubMed: 18776941]
25. Kortylewski M, Xin H, Kujawski M, Lee H, Liu Y, Harris T, et al. Regulation of the IL-23 and IL-12 balance by Stat3 signaling in the tumor microenvironment. Cancer Cell. 2009; 15:114–23. [PubMed: 19185846]
26. Renan MJ, Dowman PI. Increased radioresistance of tumor cells exposed to metallothionein-inducing agents. Radiation research. 1989; 120:442–55. [PubMed: 2594966]
27. Klinman DM, Gursel I, Klaschik S, Dong L, Currie D, Shirota H. Therapeutic potential of oligonucleotides expressing immunosuppressive TTAGGG motifs. Ann N Y Acad Sci. 2005; 1058:87–95. [PubMed: 16394128]
28. Weis SM, Cheresh DA. Tumor angiogenesis: molecular pathways and therapeutic targets. Nat Med. 2011; 17:1359–70. [PubMed: 22064426]
29. Yu H, Kortylewski M, Pardoll D. Crosstalk between cancer and immune cells: role of STAT3 in the tumour microenvironment. Nat Rev Immunol. 2007; 7:41–51. [PubMed: 17186030]
30. Kawai T, Akira S. The role of pattern-recognition receptors in innate immunity: update on Toll-like receptors. Nat Immunol. 2010; 11:373–84. [PubMed: 20404851]

NIH-PA Author Manuscript

NIH-PA Author Manuscript

NIH-PA Author Manuscript

31. Krieg AM. CpG still rocks! Update on an accidental drug. Nucleic acid therapeutics. 2012; 22:77–89. [PubMed: 22352814]
32. Heinrich PC, Behrmann I, Haan S, Hermanns HM, Muller-Newen G, Schaper F. Principles of interleukin (IL)-6-type cytokine signalling and its regulation. Biochem J. 2003; 374:1–20. [PubMed: 12773095]
33. Kortylewski M, Kujawski M, Wang T, Wei S, Zhang S, Pilon-Thomas S, et al. Inhibiting Stat3 signaling in the hematopoietic system elicits multicomponent antitumor immunity. Nat Med. 2005; 11:1314–21. [PubMed: 16288283]
34. Bosco MC, Puppo M, Blengio F, Fraone T, Capello P, Giovarelli M, et al. Monocytes and dendritic cells in a hypoxic environment: Spotlights on chemotaxis and migration. Immunobiology. 2008; 213:733–49. [PubMed: 18926289]
35. Kortylewski M, Swiderski P, Herrmann A, Wang L, Kowolik C, Kujawski M, et al. In vivo delivery of siRNA to immune cells by conjugation to a TLR9 agonist enhances antitumor immune responses. Nat Biotechnol. 2009; 27:925–32. [PubMed: 19749770]
36. Formenti SC, Demaria S. Radiation therapy to convert the tumor into an in situ vaccine. International journal of radiation oncology, biology, physics. 2012; 84:879–80.
37. Huang Q, Li F, Liu X, Li W, Shi W, Liu FF, et al. Caspase 3-mediated stimulation of tumor cell repopulation during cancer radiotherapy. Nat Med. 2011; 17:860–6. [PubMed: 21725296]
38. Zhang Q, Raoof M, Chen Y, Sumi Y, Sursal T, Junger W, et al. Circulating mitochondrial DAMPs cause inflammatory responses to injury. Nature. 2010; 464:104–7. [PubMed: 20203610]
39. Oka T, Hikoso S, Yamaguchi O, Taneike M, Takeda T, Tamai T, et al. Mitochondrial DNA that escapes from autophagy causes inflammation and heart failure. Nature. 2012; 485:251–5. [PubMed: 22535248]
40. Shatz M, Menendez D, Resnick MA. The human TLR innate immune gene family is differentially influenced by DNA stress and p53 status in cancer cells. Cancer Res. 2012; 72:3948–57. [PubMed: 22673234]
41. McKelvey KJ, Highton J, Hessian PA. Cell-specific expression of TLR9 isoforms in inflammation. Journal of autoimmunity. 2011; 36:76–86. [PubMed: 21115235]
42. Apetoh L, Ghiringhelli F, Tesniere A, Criollo A, Ortiz C, Liderau R, et al. Toll-like receptor 4-dependent contribution of the immune system to anticancer chemotherapy and radiotherapy. Nat Med. 2007; 13:1050–9. [PubMed: 17704786]
43. Tian J, Avalos AM, Mao SY, Chen B, Senthil K, Wu H, et al. Toll-like receptor 9-dependent activation by DNA-containing immune complexes is mediated by HMGB1 and RAGE. Nat Immunol. 2007; 8:487–96. [PubMed: 17417641]
44. Grivennikov SI, Karin M. Dangerous liaisons: STAT3 and NF-kappaB collaboration and crosstalk in cancer. Cytokine Growth Factor Rev. 2009; 21:11–9. [PubMed: 20018552]
45. Klaschik S, Tross D, Klinman DM. Inductive and suppressive networks regulate TLR9-dependent gene expression in vivo. J Leukoc Biol. 2009; 85:788–95. [PubMed: 19179452]
46. Zabuawala T, Taffany DA, Sharma SM, Merchant A, Adair B, Srinivasan R, et al. An ets2-driven transcriptional program in tumor-associated macrophages promotes tumor metastasis. Cancer Res. 2010; 70:1323–33. [PubMed: 20145133]
47. Gautier EL, Shay T, Miller J, Greter M, Jakubzick C, Ivanov S, et al. Gene-expression profiles and transcriptional regulatory pathways that underlie the identity and diversity of mouse tissue macrophages. Nat Immunol. 2012; 13:1118–28. [PubMed: 23023392]
48. Nolan DJ, Ciarrocchi A, Mellick AS, Jaggi JS, Bambino K, Gupta S, et al. Bone marrow-derived endothelial progenitor cells are a major determinant of nascent tumor neovascularization. Genes Dev. 2007; 21:1546–58. [PubMed: 17575055]
49. Brody JD, Ai WZ, Czerwinski DK, Torchia JA, Levy M, Advani RH, et al. In Situ Vaccination With a TLR9 Agonist Induces Systemic Lymphoma Regression: A Phase I/II Study. J Clin Oncol. 2010; 28:4324–32. [PubMed: 20697067]
50. Nechaev S, Gao C, Moreira D, Swiderski P, Jozwiak A, Kowolik CM, et al. Intracellular processing of immunostimulatory CpG-siRNA: Toll-like receptor 9 facilitates siRNA dicing and endosomal escape. J Control Release. 2013; 170:307–15. [PubMed: 23777886]

NIH-PA Author Manuscript

NIH-PA Author Manuscript

NIH-PA Author Manuscript

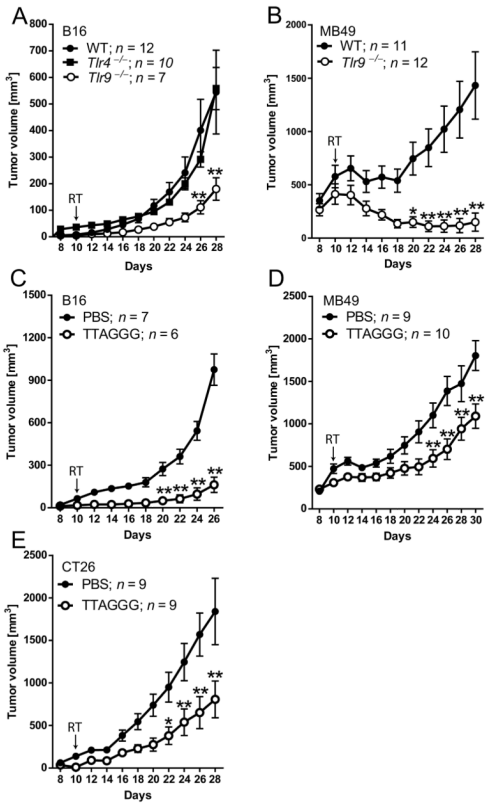

Figure 1. TLR9 activity in the tumor microenvironment accelerates tumor recurrence after local irradiation

(A) B16 tumor growth in WT, *Tlr4*$^{-/-}$ and *Tlr9*$^{-/-}$ mice after single dose of RT at 10d after tumor injection. (B) MB49 tumor growth in WT and *Tlr9*$^{-/-}$ mice after irradiation. (C–E) Blocking *Tlr9* by TTAGGG inhibits tumor relapse post-RT. WT mice were implanted subcutaneously with 1×10^5 B16 (C), 1×10^6 MB49 (D) or 5×10^5 CT26 cells (E). Tumor-bearing mice were locally irradiated and *i.v.* injected with TTAGGG or PBS every other day, starting at 10d. Data shown are from one representative of two independent experiments using 8–10 mice per group; means ± SEM. Statistically significant differences between three (A) or two (B–E) treatment groups are indicated by asterisks; RT, tumor irradiation.

NIH-PA Author Manuscript
NIH-PA Author Manuscript
NIH-PA Author Manuscript

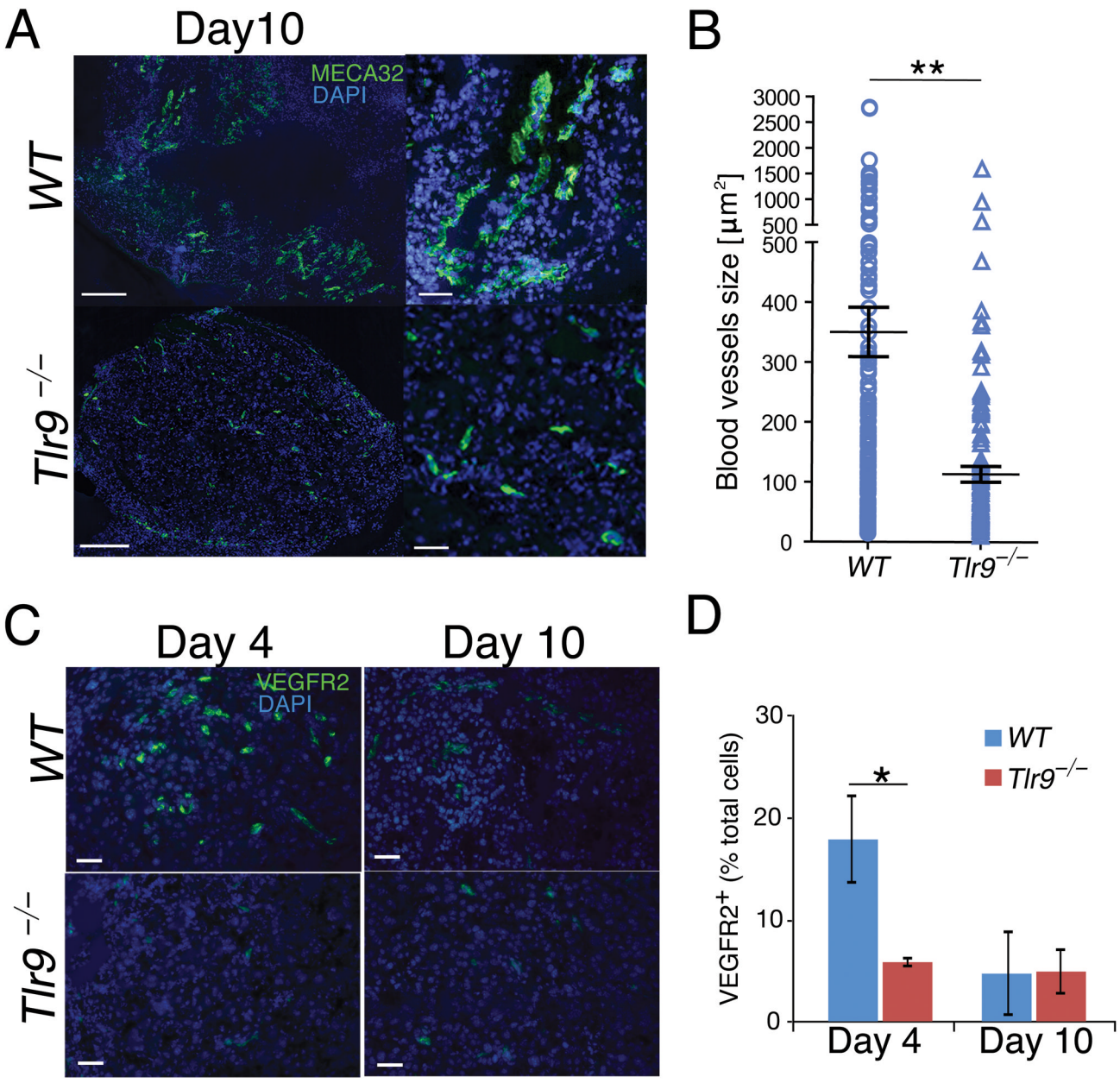

Figure 2. Lack of TLR9 expression inhibits recruitment of EPCs and tumor re-vascularization

(A) Immunofluorescent staining for tumor blood vessels using MECA32-specifc antibodies (green) and nuclear staining with DAPI (blue). Images represent whole tissue sections (left) or selected areas (right), scale bars = 200 μm or 50 μm. (B) Blood vessel assessment in whole tumor sections; shown are means ± SEM (n = 3). (C) Immunofluorescent staining of tumor-infiltrating EPCs (VEGFR2$^+$, green) 4d after radiation; scale bar = 50μm. (D) Percentages of EPCs quantified based on immunofluorescent stainings shown in Figure 2C. Shown are means ± SEM from the analysis of 3 sections/mouse.

NIH-PA Author Manuscript

NIH-PA Author Manuscript

NIH-PA Author Manuscript

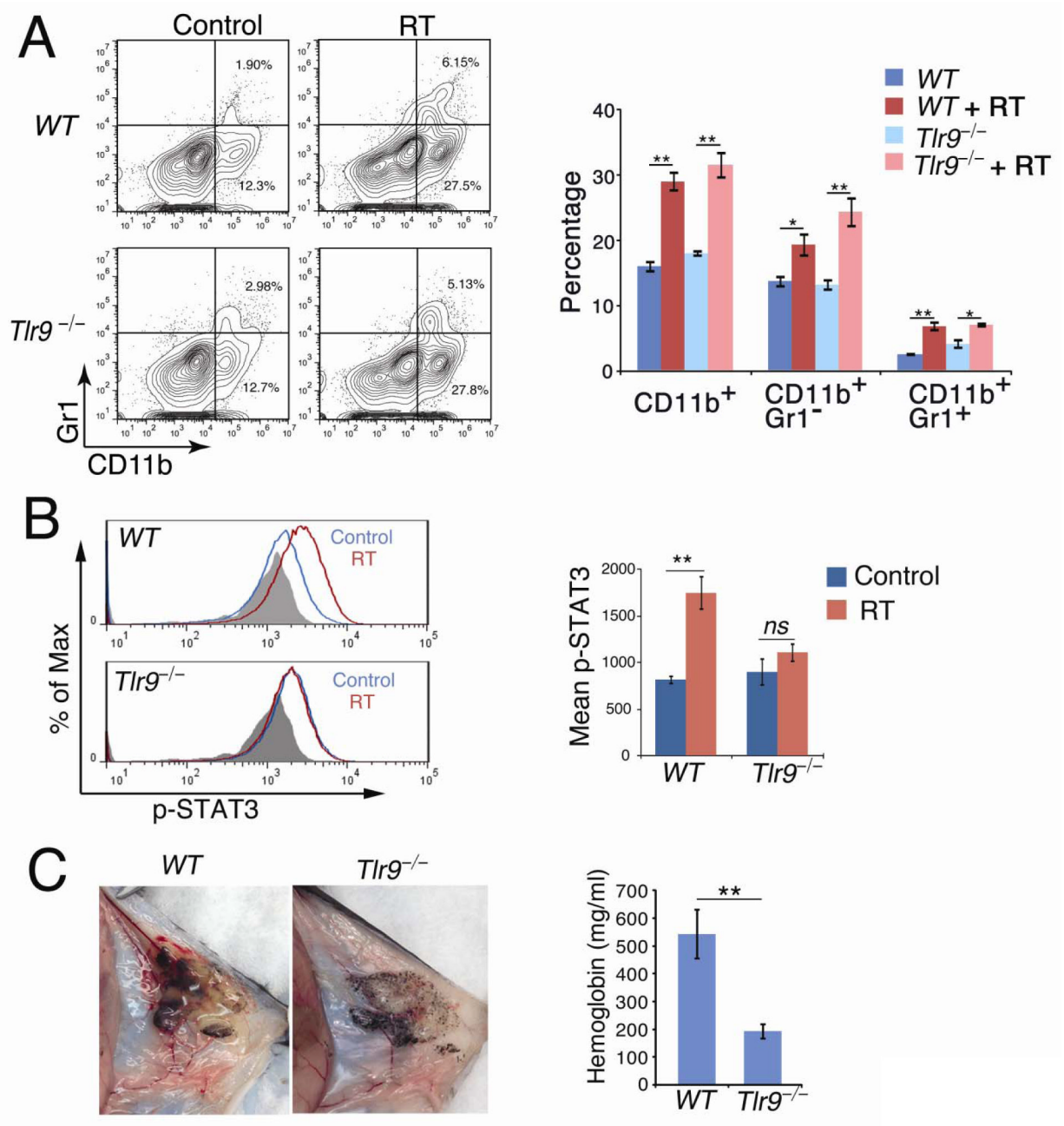

Figure 3. TLR9/STAT3 signaling in myeloid cells promotes tumor blood vessel formation post-RT

(A) Percentages of $CD11b^{+}Gr1^{-}$ and $CD11b^{+}Gr1^{+}$ myeloid populations recruited to irradiated tumors in WT and *Tlr9*$^{-/-}$mice. Flow cytometry on cell suspensions from tumors 4d after RT. Left: representative results from one of three independent experiments. Right: percentages of $CD11b^{+}$ cell populations; means ± SEM (n = 6). (B) Local RT activates STAT3 in tumor-infiltrating $CD11b^{+}Gr1^{-}$ macrophages in WT but not in *Tlr9*$^{-/-}$ mice. Left: representative results of two independent flow cytometric measurements. Right: mean fluorescence intensities (MFI) for pSTAT3 staining for all performed experiments combined; means ± SEM (n = 4). (C) Left: Matrigel plugs containing *Tlr9*$^{-/-}$ myeloid cells show a significant reduction of blood vessels. $CD11b^{+}$ cells from WT or *Tlr9*$^{-/-}$ mice were

admixed with B16 cells in Matrigel at 10:1 ratio and subcutaneously injected into WT mice. Right: hemoglobin content in Matrigel plugs at 7d; means ± SEM (n = 5).

NIH-PA Author Manuscript
NIH-PA Author Manuscript
NIH-PA Author Manuscript

NIH-PA Author Manuscript

NIH-PA Author Manuscript

NIH-PA Author Manuscript

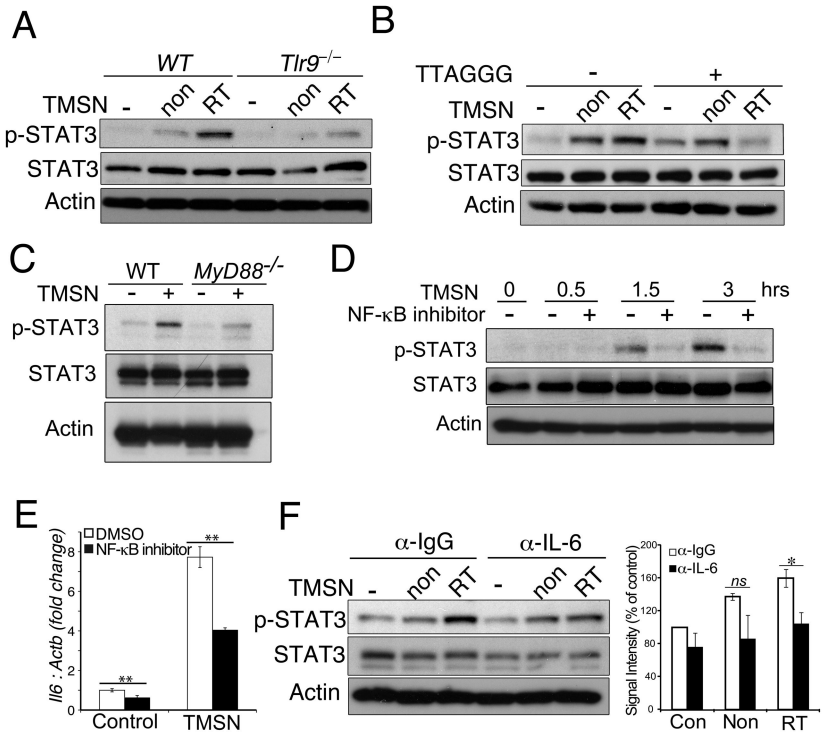

Figure 4. Tumor damage by radiation triggers TLR9/MyD88-mediated IL-6 expression and STAT3 activation

(A) *Tlr9* deletion inhibits STAT3 phosphorylation in splenocytes treated with supernatants (TMSN) from *in vivo* irradiated (RT) or not irradiated (non) B16 tumors. Total splenocytes from WT or *Tlr9*$^{-/-}$ mice were treated using different TMSNs or left untreated for 3h. Total cellular lysates were examined by WB for pSTAT3 and total STAT3 levels. (B) TLR9 antagonist (TTAGGG; 1 μM) blocks STAT3 activation in WT splenocytes treated with irradiated but not control TMSN, prepared as in Figure 4A. (C) *MyD88* gene ablation prevents STAT3 activation in myeloid cells treated with TMSN from *in vivo* irradiated B16 tumors. Splenic CD11b^{+} cells isolated from WT or *MyD88*$^{-/-}$ mice were treated using TMSN or left untreated for 3h, then pSTAT3/total STAT3 levels were examined. (D) Blocking NF-κB in myeloid cells abrogates STAT3 activation by irradiated TMSN. Splenic CD11b^{+} cells were pre-incubated for 0.5h with transcriptional NF-κB inhibitor, then treated as indicated and analyzed for STAT3 activity. (E) NF-κB inhibition prevents *Il6* upregulation by irradiated TMSN in CD11b^{+} myeloid cells. Splenic CD11b^{+} cells were treated using TMSN with or without the NF-κB inhibitor as in Figure 4D for 1.5h. Shown are the qPCR results normalized to *Actb* expression; *Il6* mRNA level in control group was set as 1. (F) IL-6 neutralization abrogates STAT3 activation by irradiated but not by control TMSN. Total splenocytes were incubated with TMSNs in the presence of IL-6-neutralizing or control IgG antibodies. Left: the representative results of the WB for pSTAT3; right: densitometric quantification of 3 independent experiments using ImageJ software (v. 1.47h). Shown are representative results from one of three (A, B, F) or two (C, D, E) independent experiments; β-actin was used as a loading control.

NIH-PA Author Manuscript

NIH-PA Author Manuscript

NIH-PA Author Manuscript

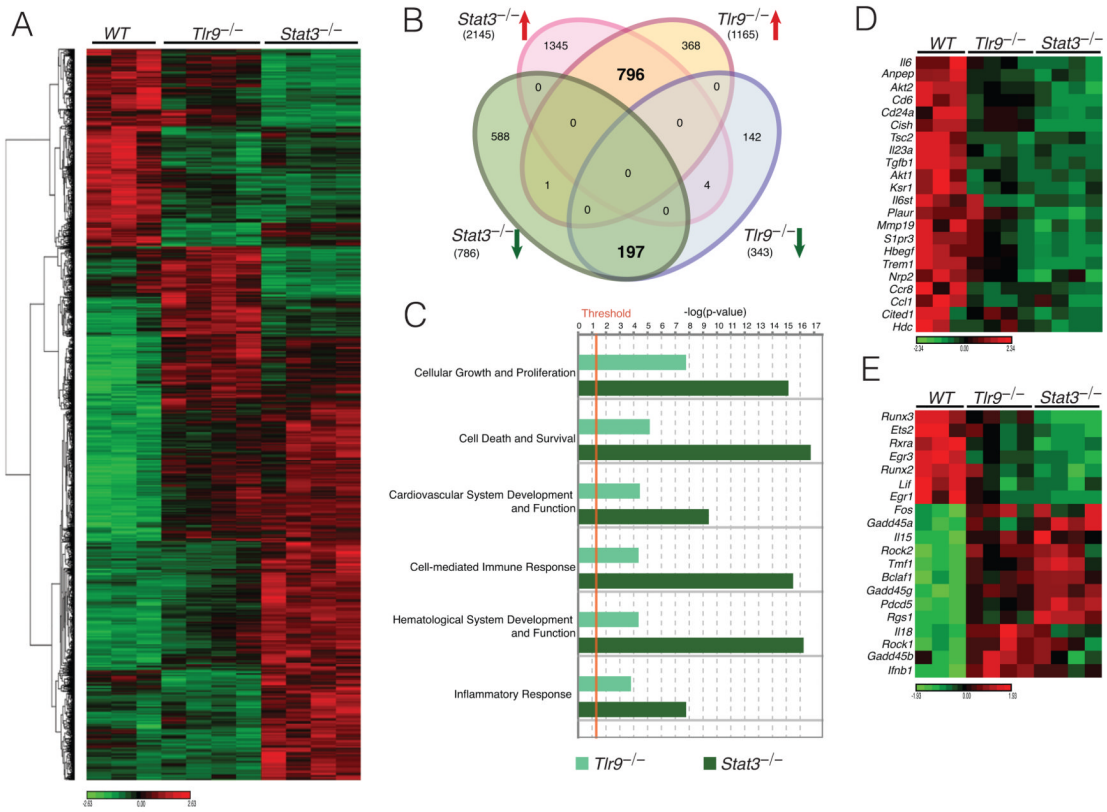

Figure 5. TLR9/STAT3 signaling modulates global gene expression in tumor-infiltrating myeloid cells after RT

(A) Overview of the gene expression pattern in the hierarchical clustering analysis. The red or green color indicates up- or downregulated expression, respectively. (B) The number of commonly regulated genes is shown using Venn diagram comparing *Tlr9*$^{-/-}$ to WT and *Stat3*$^{-/-}$ to WT groups. (C) Top functional down-regulated gene targets in *Tlr9*$^{-/-}$ and *Stat3*$^{-/-}$ compared to WT as assessed by IPA analysis. (D–E) Heatmaps showing differentially expressed genes related to angiogenesis (D) or myeloid cell differentiation (E).

NIH-PA Author Manuscript

NIH-PA Author Manuscript

NIH-PA Author Manuscript

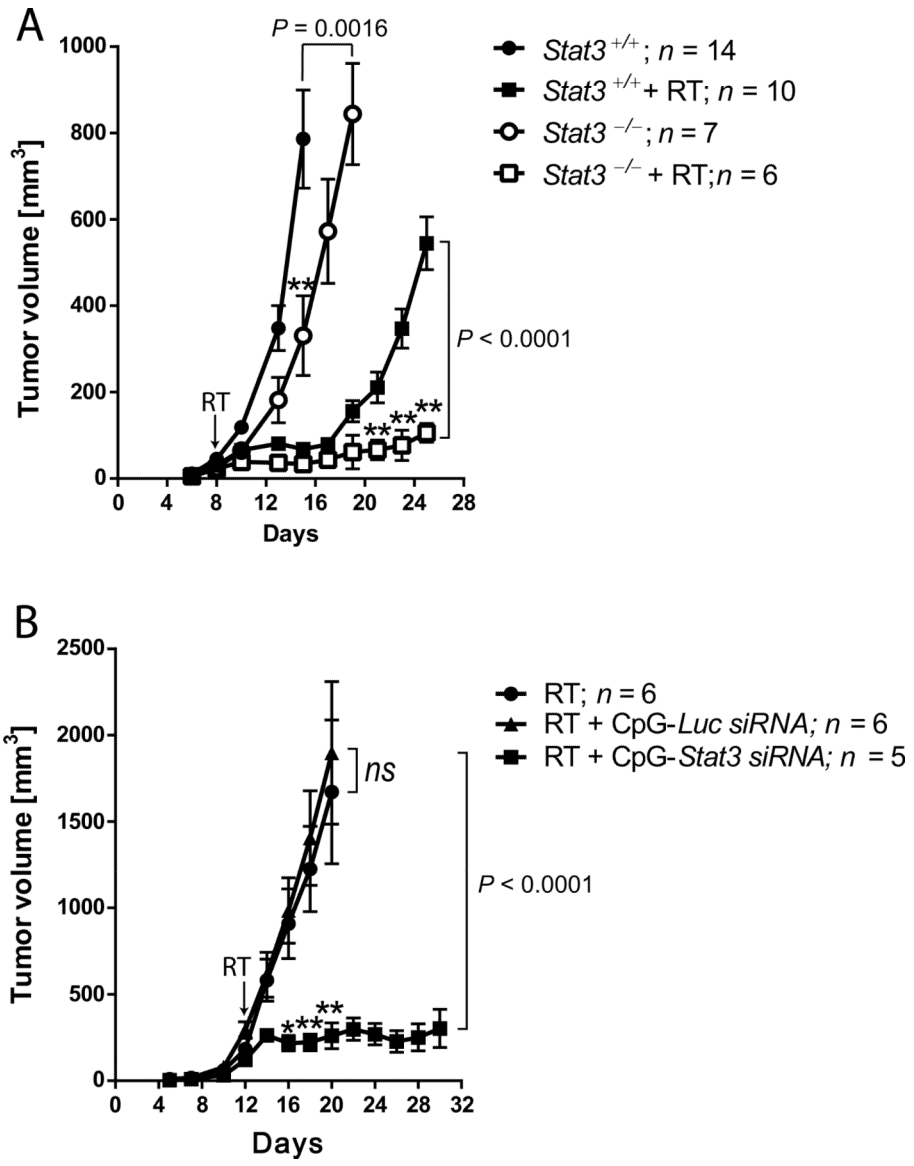

Figure 6. Targeting STAT3 in myeloid cells *in vivo* prevents B16 tumor recurrence after local irradiation

(A) B16 tumors established in mice with *Stat3*$^{+/+}$ or *Stat3*$^{-/-}$ myeloid cells were irradiated at 8d or left untreated. Representative results from one of three experiments; means ± SEM; *P =0.0016 (Stat3*$^{+/+}$ *vs. Stat3*$^{-/-}$*), P < 0.0001 (Stat3*$^{+/+}$*+RT vs. Stat3*$^{-/-}$*+RT), P < 0.0001 (Stat3*$^{+/+}$*vs. Stat3*$^{+/+}$*+RT), P = 0.054 (Stat3*$^{-/-}$ *vs. Stat3*$^{-/-}$*+RT).* (B) *Stat3* silencing in myeloid cells prevents tumor regrowth after RT. WT mice with established B16 tumors were injected intratumorally with CpG-siRNAs every other day starting at 10d or left untreated. Tumors were irradiated at 12d as indicated. Results represent one of two independent experiments; means ± SEM.

NIH-PA Author Manuscript

NIH-PA Author Manuscript

NIH-PA Author Manuscript

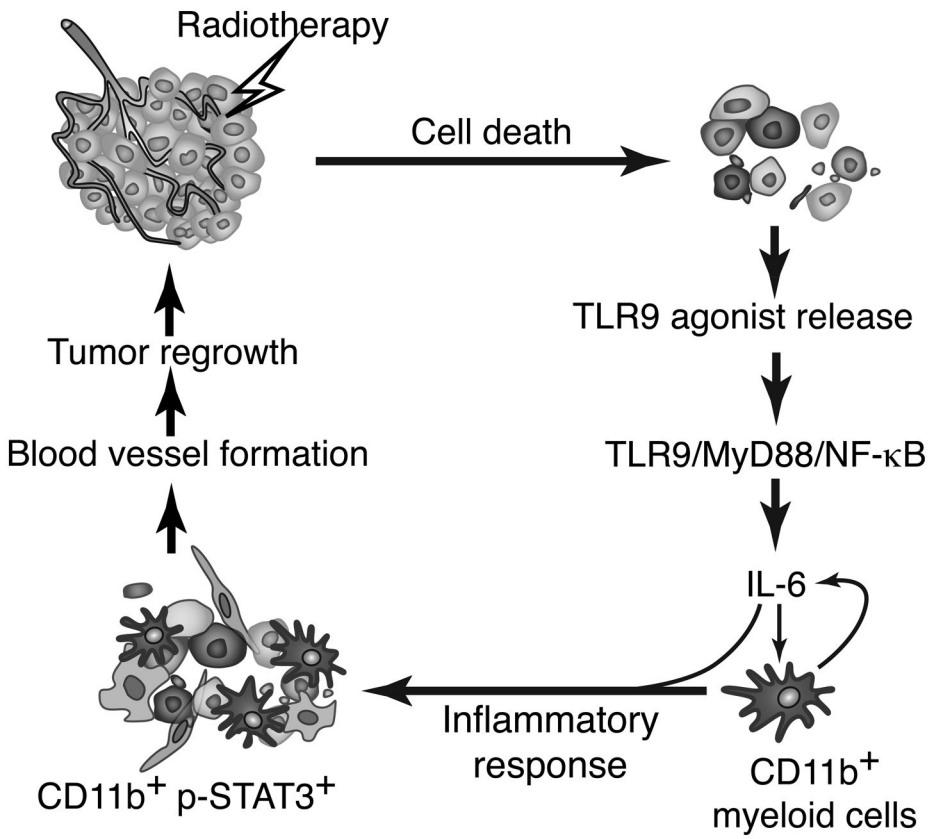

Figure 7. TLR9 triggering jump-starts STAT3 activity in myeloid cells to promote tumor recurrence after RT

Tumor irradiation generates soluble TLR9 agonists that are recognized by $CD11b^+/TLR9^+$ myeloid cells. TLR9 signals through MyD88 and NF-κB to induce IL-6 expression. IL-6 initially becomes a major trigger of tumorigenic STAT3 activity in myeloid cells and potentially other cell populations. Immature $TLR9^+/pSTAT3^+$ myeloid cells promote formation of blood vessels, thereby accelerating tumor recurrence.